ORIGINAL ARTICLE

AASLD
AMERICAN ASSOCIATION FOR
THE STUDY OF LIVER DISEASES

OPEN

Quantitative fibrosis identifies biliary tract involvement and is associated with outcomes in pediatric autoimmune liver disease

Leticia Khendek[1,2] 🄳 | Cyd Castro-Rojas[1,2] | Constance Nelson[1,2] 🄳 | Mosab Alquraish[1,2] | Rebekah Karns[2,3] 🄳 | Jennifer Kasten[4] 🄳 | Xiao Teng[5] | Alexander G. Miethke[1,2,6] 🄳 | Amy E. Taylor[1,2,6] 🄳

[1]Department of Pediatrics, Division of Gastroenterology, Hepatology, and Nutrition, Cincinnati Children's Hospital Medical Center, Cincinnati, Ohio, USA

[2]Center for Autoimmune Liver Disease (CALD), Cincinnati Children's Hospital Medical Center, Cincinnati, Ohio, USA

[3]Department of Pediatrics, Division of Biostatistics and Epidemiology, Cincinnati Children's Hospital Medical Center, Cincinnati, Ohio, USA

[4]Department of Pediatrics, Division of Pathology, Cincinnati Children's Hospital Medical Center, Cincinnati, Ohio, USA

[5]HistoIndex Pte Ltd, Singapore, Singapore

[6]Department of Pediatrics, University of Cincinnati College of Medicine, Cincinnati, Ohio, USA

Correspondence
Leticia Khendek, Department of Pediatrics, Division of Pediatric Gastroenterology, Hepatology and Nutrition, Cincinnati Children's Hospital Medical Center, 3333 Burnet Ave, Cincinnati, OH 45229, USA.
Email: leticia.khendek@umontreal.ca

Abstract

Background: Children with autoimmune liver disease (AILD) may develop fibrosis-related complications necessitating a liver transplant. We hypothesize that tissue-based analysis of liver fibrosis by second harmonic generation (SHG) microscopy with artificial intelligence analysis can yield prognostic biomarkers in AILD.

Methods: Patients from single-center studies with unstained slides from clinically obtained liver biopsies at AILD diagnosis were identified. Baseline demographics and liver biochemistries at diagnosis and 1 year were collected. Clinical endpoints studied included the presence of varices, variceal bleeding, ascites, HE, and liver transplant. In collaboration with HistoIndex, unstained slides underwent SHG/artificial intelligence analysis to map fibrosis according to 10 quantitative fibrosis parameters based on tissue location, including total, periportal, perisinusoidal, and pericentral area and length of strings.

Results: Sixty-three patients with AIH (51%), primary sclerosing cholangitis (30%), or autoimmune sclerosing cholangitis (19%) at a median of 14 years old (range: 3–24) were included. An unsupervised analysis of quantitative fibrosis parameters representing total and portal fibrosis identified a patient cluster with more primary sclerosing cholangitis/autoimmune sclerosing cholangitis. This group had more fibrosis at diagnosis by METAVIR classification of histopathological review of biopsies (2.5 vs. 2; $p = 0.006$). This

---

Abbreviations: AI, artificial intelligence; AIH, autoimmune hepatitis; AILD, autoimmune liver disease; ASC, autoimmune sclerosing cholangitis; IgG, immunoglobulin G; MASLD, metabolic dysfunction–associated steatotic liver disease; MRCP, magnetic resonance cholangiopancreatography; NumStr, number of strings; PC, principal component; PctSHG, percent second harmonic generation; PSC, primary sclerosing cholangitis; qFibrosis, quantitative fibrosis; SHG, second harmonic generation; StrArea, string area; StrAreaCV, string area central vein; StrAreaPS, string area perisinusoidal space; StrAreaPT, string area portal tract; StrLength, string length; StrLengthCV, string length central vein; StrLengthPS, string length perisinusoidal space; StrLengthPT, string length portal tract; TPEF, two-photon excited fluorescence.

Supplemental Digital Content is available for this article. Direct URL citations are provided in the HTML and PDF versions of this article on the journal's website, www.hepcommjournal.com.

- -

quantitative fibrosis pattern also predicted abnormal 12-month ALT with an OR of 3.6 (1.3–10, p = 0.014), liver complications with an HR of 3.2 (1.3–7.9, p = 0.01), and liver transplantation with an HR of 20.1 (3–135.7, p = 0.002).

Conclusions: The application of SHG/artificial intelligence algorithms in pediatric-onset AILD provides improved insight into liver histopathology through fibrosis mapping. SHG allows objective identification of patients with biliary tract involvement, which may be associated with a higher risk for refractory disease.

Keywords: autoimmune hepatitis, autoimmune sclerosing cholangitis, biomarker, liver fibrosis, primary sclerosing cholangitis

INTRODUCTION

Autoimmune liver disease (AILD) is a spectrum of diseases that include autoimmune hepatitis (AIH) and primary sclerosing cholangitis (PSC). Pediatric patients affected with AILD are at risk of progressive fibrosis evolving to end-stage liver disease requiring liver transplantation before adulthood.[1,2] AIH can be aggressive in children and adolescents, with up to a third of patients presenting with cirrhosis at diagnosis and relapse occurring in up to 40% of patients despite treatment, usually at the time of steroid weaning.[3,4] A unique feature of AILD in children is the co-occurrence of AIH and PSC in patients, which is referred to as autoimmune sclerosing cholangitis (ASC). Children with ASC have a worse prognosis than AIH, and treatments are not effective in preventing the progression of bile duct damage in nearly 50% of patients.[5] For children with PSC, there are currently no disease-modifying treatments other than liver transplant. In a multicenter cohort of 781 pediatric patients with PSC, nearly 30% had an adverse liver-related outcome, and 14% underwent liver transplantation at a median of 4 years from diagnosis.[6] Hence, clinical trials to develop better therapies for pediatric AILD are a pressing need.

Consensus guidelines recommend using multiple surrogate biomarkers—circulating, imaging, and histologic—for prognostic purposes in both clinical care and trial development.[7,8] In pediatric PSC, normalization of GGT levels over the first year of diagnosis was shown to be associated with less adverse liver-related outcomes.[9] However, similarly to ALP in adult PSC, it is possible that GGT fluctuates over the course of the disease.[10] In terms of imaging modalities, quantitative magnetic resonance cholangiopancreatography (MRCP) parameters have been used to differentiate AIH from PSC/ASC.[11] MRCP scores have also been shown to be predictive of PSC complications.[12] In AIH, while biomarkers are currently still lacking, ongoing research on new antibodies and metabolomic profiling may serve to develop future treatments.[13]

Second harmonic generation (SHG) microscopy combined with two-photon excited fluorescence (TPEF) is recently being used to accurately quantify fibrillar collagen.[14] SHG microscopy allows the identification of type 1 and 3 collagen fibers as photons interact with their non-centrosymmetric structure, while TPEF allows to capture the background liver parenchyma.[15,16] A computerized algorithm is then used to localize and quantify fibrosis from the generated images. This new technique has the advantages of less interobserver variability, more precision as fibrosis is graded on a continuous rather than a semi-quantitative scale, and less variation from the staining process. This method has been validated in adult metabolic dysfunction–associated steatotic liver disease (MASLD) and chronic hepatitis B infection.[17,18] Moreover, in a recent phase 2 trial, SHG captured perisinusoidal fibrosis regression that traditional microscopy and established fibrosis scores did not in patients with MASLD treated with a non-bile acid farnesoid X receptor agonist.[19] These findings demonstrate the potential role of SHG in clinical trials and the development of new therapies.

SHG-based fibrosis assessment has not been studied and applied to pediatric AILD to improve the predictive performance of liver histopathology. In this study, we hypothesize that SHG microscopy with artificial intelligence (AI) analysis of liver biopsy tissue will reveal fibrosis patterns and serve as a *prognostic biomarker* associated with clinical outcomes in pediatric AILD.

METHODS

Study design and population

Patients who had clinical liver biopsy tissue available from the time of AILD diagnosis were identified

from 1 prospective single-center cohort study (NCT03178630; IRB ID: 2016-7388) and 1 retrospective single-center cohort study (IRB ID: 2021-0196). Patients < 25 years of age were enrolled in the study following written informed consent with study protocols approved by the Institutional Review Board (ID: 2016-7388). For patients from the retrospective study, a waiver of informed consent was obtained (IRB ID: 2021-0196). The study protocols conformed to the ethical guidelines of the 1975 Declaration of Helsinki. Baseline demographics, including sex, age, AILD diagnosis, and concurrent inflammatory bowel disease diagnosis, were recorded. Liver biochemistries, which included ALT, AST, GGT, and ALP at the time of diagnosis and at 12 months (± 3 mo), were collected. Subjects whose follow-up data were outside these bounds were excluded from the follow-up analysis but were included in the baseline cohort description. See Supplemental Figure S1, http://links. lww.com/HC9/B154, for a flowchart that illustrates the inclusion and exclusion criteria for our cohort. Abnormal values were determined based on laboratory-age-sex–determined reference ranges. Other baseline laboratory values recorded included international normalized ratio, total bilirubin, MELD score, IgG, and auto-antibody titers (antinuclear antibody, smooth muscle antibody, and liver kidney microsomal type 1 antibody). Simplified Autoimmune Hepatitis Score was calculated for each patient at the time of diagnosis.[20] MRCP and endoscopic retrograde cholangiopancreatography results were recorded in patients who underwent these. The diagnosis of AIH, ASC, or PSC was made clinically by the treating physician. Liver-related clinical endpoints studied over patients' entire follow-up included the presence of esophageal varices on endoscopy, episodes of variceal bleeding, development of ascites (defined by finding on imaging or the start of diuretic treatment), HE (defined as a clinical episode or start of treatment with rifaximin or lactulose), listing for liver transplantation, and undergoing liver transplantation. Liver transplantation was also studied as an independent outcome.

Histological assessment

Hematoxylin and eosin and trichrome-stained slides from clinical liver biopsies at diagnosis were consecutive to the unstained slides subjected to SHG/AI. Stained slides were reviewed by a pathologist (Jennifer Kasten) who was blinded to clinical and SHG information. Each biopsy was assessed for the severity of fibrosis according to METAVIR classification and Ishak stage, modified Ishak Histologic Activity Index, and bile duct damage (pericholangitis, periductal fibrosis, and ductal proliferation).[21–23]

Quantitative fibrosis

Unstained liver specimens from paraffin-embedded clinical liver biopsy tissue at the time of AILD diagnosis underwent SHG/TPEF and AI analysis to map and quantify collagen at HistoIndex (Singapore), as previously reported.[14] This included SHG/TPEF imaging of biopsies using a Genesis system by stitching image tiles of a dimension of 200×200 μm^2 and AI-based analysis. For liver biopsy specimens to be included, they needed to measure 20 mm in length, 4 mm in width, and 4–5 μm in thickness. Three separate regions (portal tract space, perisinusoidal space, and central vein space) were differentiated, namely by their number of vessels and the presence of bile ducts, and distinguished from each other by a classification and regression tree method. Quantitative features (eg, number of strings) were then extracted from aggregated and distributed collagen for a total of 10 quantitative fibrosis (qFibrosis) variables. These variables included overall fibrosis (Percent SHG [PctSHG], Number of Strings [NumStr], String Area [StrArea], and String Length [StrLength]), portal tract fibrosis (String Area Portal Tract [StrAreaPT] and String Length Portal Tract [StrLengthPT]), perisinusoidal fibrosis (String Area Perisinusoidal Space [StrAreaPS] and String Length Perisinusoidal Space [StrLengthPS]), and perivenular fibrosis (String Area Central Vein [StrAreaCV] and String Length Central Vein [StrLengthCV]).

Statistical analyses

Data are presented as count or median with range. Nonparametric testing (Wilcoxon rank sum test) and Fisher Exact tests were used to determine if continuous and categorical clinical variables differed significantly between AILD groups. All qFibrosis values underwent a logarithmic transformation, were baselined to the median of all samples (the median was subtracted from each subject's observed value for each qFibrosis variable), and were submitted for pairwise Spearman correlation analysis. To identify patient clustering based on fibrosis patterns, qFibrosis parameters were submitted to hierarchical clustering analysis. The hierarchical clustering used the Euclidean measure to obtain the distance matrix and complete agglomeration method for clustering, which identified 2 patient subgroups. Based on clustering results, patients were assigned to hierarchical clusters A or B. To determine if clinical variables differed significantly between the patient clusters, nonparametric testing (Wilcoxon) and Fisher Exact tests were used as appropriate. The association between hierarchical clusters and biochemistries at 12 months and other clinical endpoints was assessed using logistic regression. We performed survival analysis using a Cox proportional hazards model to assess

the difference in time to any complication between histoclusters A and B.

Due to the correlation structure of the qFibrosis variables, a principal component (PC) analysis was conducted to quantitatively describe the relationships between qFibrosis variables. Each PC is a linear combination of all qFibrosis parameters. A "factor loading" is computed for each qFibrosis parameter, which gives it an appropriate weight for each PC. The first PC accounts for the largest proportion of variability in the data, with each subsequent component decreasing in variability explained. Only PC 1–3, which account for >80% of variability, were included in further analysis. We considered qFibrosis factor loadings of >0.3 or <−0.3 to indicate that a qFibrosis parameter was relevant to that PC. The Spearman correlation between the 3 PC and established histological fibrosis scores (METAVIR classification and Ishak stages) was computed. Logistic regression analysis was performed

to assess the association between each PC and biochemistries at 12 months, and Cox proportional hazards regression was performed to assess the association between each PC and time-to-complication.

Graphs were generated with Rv4.2.2, and the PC analysis was performed in SASv9.4.

RESULTS

To determine if qFibrosis at the time of diagnosis could be used to identify fibrosis patterns and was associated with prognosis, SHG microscopy with TPEF and AI analysis were performed on liver biopsies of 63 patients at diagnosis. Median time of follow-up was 5.6 years (0.3–16 years). Patients' demographic information, as well as the severity of their liver injury by liver biochemistries and fibrosis scores, are summarized in Table 1. Half of the cohort had a diagnosis of AIH.

TABLE 1 Patient demographics, liver biochemistries, and histopathologic scores

|	AIH (n = 32)	ASC (n = 12)	PSC (n = 19)
Age, median (range)	13 (3–24)	13 (3–17)	15 (3–19)
Sex: female, n (%)	15 (47)	6 (50)	11 (58)
Race: White, n (%)	29 (91)	10 (83)	18 (95)
Ethnicity: non-Hispanic, n (%)	31 (97)	11 (92)	19 (100)
IBD, n (%)	3 (9)	9 (75)	16 (84)
Simplified IAIHG score:			
Score, median (range)	6 (3–8)	6.5 (3–8)	3 (2–7)
% with ≥6	78	75	16
IgG, median (range)	1680 (356–5170)	2270 (795–3420)	1650 (1146–3680)
Cholangiopathy on MRCP/ERCP, % (n, patient with imaging)	0 (n = 14)	100% (n = 12)	100% (n = 15)
Liver function at BL, median (range)			
INR	1.27 (1.03–3.69)	1.08 (0.9–1.76)	1.03 (0.84–1.92)
Total bilirubin (mg/dL)	1.65 (0.1–26.5)	0.6 (0.3–1)	0.35 (0.2–1.8)
MELD	12 (7–27)	7 (6–13)	7 (6–16)
Serum liver biochemistries at BL, median (range; U/L)			
ALT	268 (48–2814)	119 (29–501)	128 (17–490)
AST	280 (33–2985)	102 (29–528)	89 (9–472)
ALP	263 (56–886)	615 (75–1402)	332 (46–1163)
GGT	101 (10–338)	368 (20–796)	355 (29–890)
Histopathology, median (range)			
Number of biopsies scored	AIH (n = 31)	ASC (n = 11)	PSC (n = 18)
METAVIR classification	2 (0–4)	2 (1–3)	1.5 (0–4)
Ishak stage	3 (1–6)	3 (1–5)	2 (0–5)
HAI score	10 (0–18)	5 (1–11)	1.5 (0–13)
Bile duct damage, n (%)			
Pericholangitis	14 (45)	9 (82)	10 (56)
Periductal fibrosis	4 (13)	8 (73)	14 (74)
Ductal proliferation	18 (58)	9 (82)	11 (61)

Abbreviations: AIH, autoimmune hepatitis; ASC, autoimmune sclerosing cholangitis; BL, baseline; ERCP, endoscopic retrograde cholangiopancreatography; HAI, Histologic Activity Index; IAIHG, International Autoimmune Hepatitis Group; IBD, inflammatory bowel disease; IgG, immunoglobulin G; INR, international normalized ratio; MRCP, magnetic resonance cholangiopancreatography; PSC, primary sclerosing cholangitis.

Patients with PSC and ASC were more likely to have concurrent inflammatory bowel disease ($p < 0.0001$). The median simplified AIH score was ≥ 6 for AIH and ASC, and 3 for PSC ($p < 0.0001$). Seven patients with AIH presented with acute liver failure or severe hepatitis and tended to have negative auto-antibody panels on initial evaluation. Patients in the PSC and ASC groups all had evidence of large duct PSC on MRCP or endoscopic retrograde cholangiopancreatography (n = 27), and if they had not undergone imaging, they had small-duct changes compatible with PSC on biopsy (n = 4). On presentation, international normalized ratio, serum total bilirubin, aminotransferase levels, and MELD score were more elevated in patients with AIH, while the cholestatic markers ALP and GGT were higher in the PSC and ASC groups compared with the other groups, respectively *(p < 0.01 by Kruskal-Wallis)*. There was no statistically significant difference between diagnoses in fibrosis severity by METAVIR classification or Ishak stage. Ishak-modified Histologic Activity Index scores were more elevated in the AIH group compared to the PSC and ASC groups ($p = 0.0001$). Patients with ASC and PSC tended to have more evidence of bile duct damage upon a systematic review of histopathology, although these features were also present in patients with AIH. Pericholangitis was most common in patients with ASC. Liver-related complications and number of liver transplants listed per diagnosis can be found in Supplemental Table S1, http://links.lww.com/HC9/B155.

In the qFibrosis analysis, the correlation between the 10 qFibrosis parameters was first assessed, and they were found to be highly correlated to each other (Supplemental Figure S2, http://links.lww.com/HC9/B156). An unsupervised hierarchical clustering analysis of qFibrosis parameters was performed to evaluate the association between qFibrosis values and AILD phenotype. Parameters clustered into 3 groups (PctSHG, StrArea, StrAreaPT, and StrLengthPT; StrAreaCV and StrLengthCV; NumStr, StrLength, StrAreaPS, and StrLengthPS). Two distinct patient clusters (clusters A and B) were observed, in which patients from cluster B had higher overall fibrosis (PctSHG and StrArea) and portal tract fibrosis (StrAreaPT and StrLengthPT) than those in cluster A (Figure 1). Clinical characteristics for patients according to cluster assignment are summarized in Table 2. Cluster B patients had more often a diagnosis of PSC or ASC ($p = 0.03$). Serum GGT and IgG levels were significantly higher ($p = 0.001$ and $p = 0.01$, respectively), and fibrosis stages by METAVIR or Ishak were more advanced in patients from cluster B compared with A ($p = 0.006$ and $p = 0.005$, respectively). Importantly, a higher percentage of patients had persistently abnormal ALT at 12 months in cluster B ($p = 0.02$). Serum GGT levels at 12 months were also higher in cluster B ($p = 0.04$). The data do not suggest a significant difference in time to complication between the 2 groups ($p = 0.63$; Supplemental Figure 3, http://links.lww.com/HC9/B157). The fibrosis patterns by SHG microscopy for patients in clusters A and B are illustrated in Figure 2.

A PC analysis was then performed with the hypothesis that the PCs would confirm the qFibrosis clustering
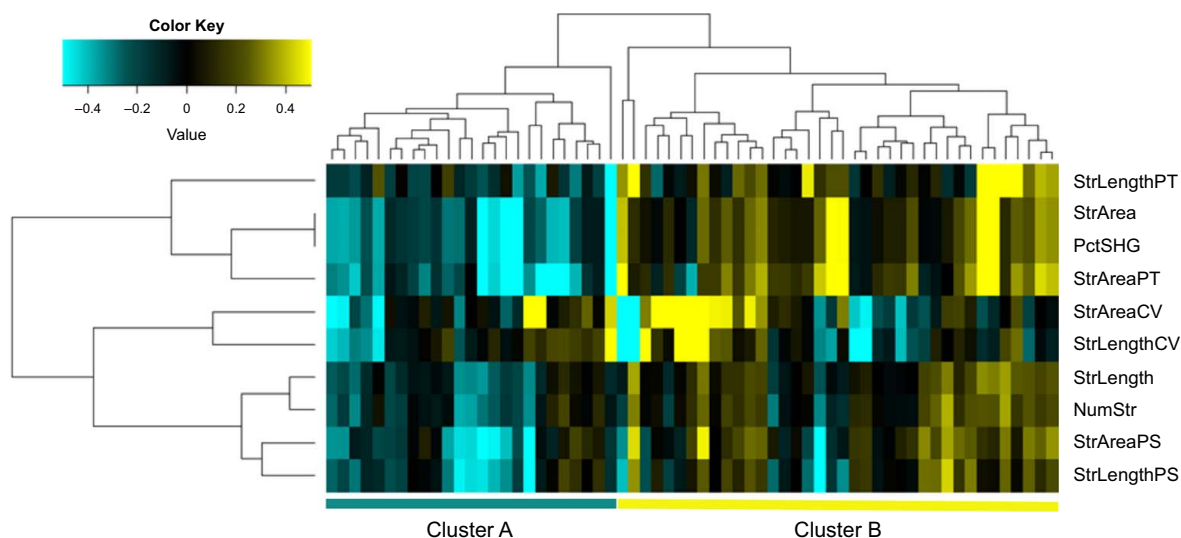
FIGURE 1 Clustering of patients according to overall fibrosis and periportal fibrosis by SHG. Unsupervised hierarchical clustering analysis of the 10 qFibrosis variables revealed 3 variable clusters: (1) PctSHG, StrArea, StrAreaPT, and StrLengthPT; (2) StrAreaCV and StrLengthCV; and (3) NumStr, StrLength, StrAreaPS, and StrLengthPS. Two distinct patient clusters (clusters A and B) were observed, where patients from cluster B had greater overall fibrosis (PctSHG and StrArea) and portal tract fibrosis (StrAreaPT and StrLengthPT) than those in cluster A. Abbreviations: NumStr, number of strings; PctSHG, percent SHG; SHG, second harmonic generation; StrArea, string area; StrAreaCV, string area central vein; StrAreaPS, string area perisinusoidal space; StrLengthPS, string length perisinusoidal space; StrAreaPT, string area portal tract; StrLength, string length; StrLengthCV, string length central vein; StrLengthPT, string length portal tract.

TABLE 2 Characteristics of patients in each histocluster

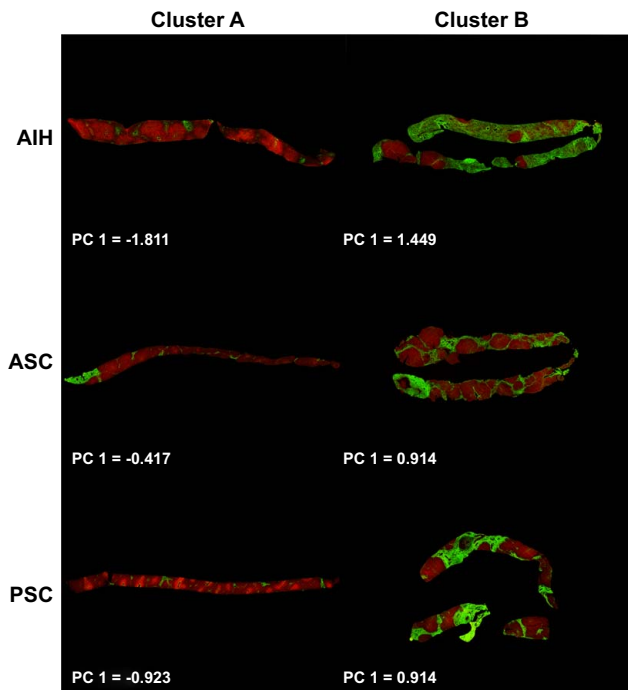|	Patients in cluster A (n = 25)	Patients in cluster B (n = 38)	p
Age, median (range)	11.5 (3–18)	13.6 (3–24)	0.62
Sex: female, n (%)	14 (56)	18 (47)	0.61
Diagnosis, n (%)			
AIH	18 (72)	14 (37)	**0.03**
PSC	4 (16)	15 (39)	
ASC	3 (12)	9 (24)	
IBD, n (%)	9 (36)	19 (50)	0.31
Liver function at BL, median (range)			
INR	1.17 (0.84–3.69)	1.12 (0.9–1.92)	0.34
Total bilirubin (mg/dL)	0.5 (0.1–26.5)	0.6 (0.2–14.2)	0.68
MELD	10 (6–27)	8 (6–23)	0.1
Serum liver biochemistries at BL, median (range; U/L)			
ALT	186 (17–2687)	162 (20–2814)	0.35
AST	128 (9–2227)	130 (33–2985)	0.54
ALP	276 (46–1009)	315 (56–1402)	0.08
GGT	76 (10–857)	235 (16–890)	**0.001**
IgG at BL, median (range; mg/dL)	1390 (356–4130)	1980 (753–5170)	**0.01**
Histopathology, median (range)			
METAVIR classification	2 (0–3)	2.5 (1–4)	**0.006**
Ishak stage	2 (0–4)	4 (0–6)	**0.005**
HAI score	4 (0–18)	7 (0–14)	0.65
Serum liver biochemistries at 12 months, median (range; U/L) n = 57			
ALT	31 (14–161)	44 (6–330)	0.16
Abnormal ALT (n, %)	2 (9)	13 (38)	**0.02**
AST	30 (13–89)	41 (11–164)	0.14
Abnormal AST (n, %)	8 (35)	20 (59)	0.1
ALP	172 (49–478)	202 (36–923)	0.48
Abnormal ALP (n, %)	3 (13)	7 (21)	0.72
GGT	17 (5–228)	38 (7–1364)	**0.04**
Abnormal GGT (n, %)	6 (26)	14 (41)	0.27
Any liver complication, n (%)	5 (20)	12 (32)	0.39
Liver transplant, n (%)	1 (4)	5 (13)	0.39

Abbreviations: AIH, autoimmune hepatitis; ASC, autoimmune sclerosing cholangitis; BL, baseline; HAI, Histologic Activity Index; IBD, inflammatory bowel disease; IgG, immunoglobulin G; INR, international normalized ratio; PSC, primary sclerosing cholangitis.
Bold values are Statistical significance of p value.

observed in hierarchical clustering and quantify the data structure of the qFibrosis variables. Three PCs accounted for >80% of variability (PC1, PC2, and PC3; Table 3). PC1 was composed of parameters reflective of overall fibrosis and portal tract fibrosis (PctSHG, StrArea, StrAreaPT, and StrLengthPT), PC2 of pericentral fibrosis (StrAreaCV and StrLengthCV), and PC3 of fibrosis from all 3 biopsy regions (NumStr, StrAreaPT, StrAreaPS, StrLengthPS, and StrAreaCV). In correlation analysis, only PC1 was found to be strongly correlated ($r > 0.6$) with both METAVIR classification and Ishak staging (Figure 3). PC1 was also strongly associated with hierarchical clusters A and B ($p < 0.0001$; Figure 4). The qFibrosis variables that comprised PC1 were the dominant variables directing subject clustering into hierarchical clusters A and B, indicating that overall and portal tract fibrosis may be most relevant in segregating phenotypes.

Logistic regression analysis was applied to determine if the PCs were associated with 12-month serum biochemistries. Only PC1 was significantly associated with outcomes (Table 4). A 1-unit increase of PC1 predicted abnormal 12-month ALT with an OR of 3.6 (1.3–10, $p = 0.01$). PC1 was comparable to METAVIR and Ishak as a predictor of abnormal ALT (OR 1.7 [1.1–2.6], $p = 0.02$; OR 2.5 [1.2–4.8], $p = 0.01$, respectively; Supplemental Table S2, http://links.lww.com/HC9/B155) at 12 months. PC1 was also

FIGURE 2 Patterns of fibrosis by SHG. SHG images of liver biopsies according to AILD diagnosis and Histocluster. Patients in cluster B have evidence of greater overall fibrosis and periportal fibrosis than patients in cluster A. PC1 value is indicated for each biopsy. Abbreviations: AILD, autoimmune liver disease; PC, principal component; SHG, second harmonic generation.

associated with AST with an OR of 3.8 (1.5–9.8, p = 0.005). In terms of clinical endpoints, using Cox proportional hazards modeling, we found that PC1 was significantly associated with event-free survival. PC1 incrementally conferred a 3-fold greater risk of

TABLE 3 The principal component analysis of qFibrosis parameters and their factor loadings

	PC1	PC2	PC3
PctSHG	0.43	0.05	−0.17
NumStr	0.17	0.16	0.37
StrArea	0.43	0.05	−0.17
StrLength	0.2	0.13	0.3
StrAreaPT	0.58	−0.09	−0.33
StrLengthPT	0.37	−0.11	−0.03
StrAreaPS	0.23	0.21	0.46
StrLengthPS	0.17	0.2	0.52
StrAreaCV	−0.05	0.71	−0.32
StrLengthCV	−0.09	0.58	−0.15

*Note*: The qFibrosis parameters included in each variable group are shaded in red.
Abbreviations: NumStr, number of strings; PC, principal component; PctSHG, percent second harmonic generation; StrArea, string area; StrAreaCV, string area central vein; StrAreaPS, string area perisinusoidal space; StrAreaPT, string area portal tract; StrLength, string length; StrLengthCV, string length central vein; StrLengthPS, string length perisinusoidal space; StrLengthPT, string length portal tract.

experiencing a liver-related complication (HR 3.2 [1.3–7.9], p = 0.01) and an over 20-fold greater risk of undergoing liver transplantation (HR 20.1 [3–135.7], p = 0.002). These results were comparable to the HR associated with METAVIR and Ishak for liver-related events (HR 2.7 [1.6, 4.5], p = 0.0002; HR 1.8 [1.3, 2.5], p = 0.0008, respectively) and liver transplantation (HR 6.4 [2, 20.7], p = 0.002; HR 2.8 [1.4, 5.7], p = 0.004, respectively). The other patterns of fibrosis associated with PC2 and PC3 did not yield significant results as predictors.

DISCUSSION

In this study, SHG microscopy with AI analysis was used to study patterns of collagen deposition in liver biopsies of patients with pediatric AILD. A pattern comprised of total and periportal fibrosis was identified and shown to perform well compared to the conventional histopathologic scores of METAVIR and Ishak staging. When applied to the cohort, it segregated patients into 2 groups, revealing 1 group with more patients with PSC/ASC and inflammatory bowel disease that were less likely to achieve biochemical remission at 1 year. This pattern of qFibrosis was also associated with adverse liver-related outcomes and liver transplantation. These data suggest that qFibrosis could serve as a useful tissue-based prognostic biomarker in AILD.

The role of SHG microscopy as a histologic tool to assess liver fibrosis is being studied in different liver diseases. This technology captures fibrillar collagen and has the advantage of not relying on tissue staining. Its ability to quantify fibrosis reliably was first shown in Hepatitis B.[18,24] Chang et al[14] have also demonstrated its use in MASLD, where it accurately evaluates the severity of fibrosis. Moreover, it has been shown to improve the inter-reader reliability of pathologists grading fibrosis severity in Metabolic dysfunction-associated steatohepatitis.[25] This is valuable as suboptimal inter-rater variability in histopathological reading can negatively impact patient selection into clinical trials as well as surrogate endpoint measurement.[26] In Metabolic dysfunction-associated steatohepatitis, digital pathology is being used in clinical trials and captures histological improvement not measured by current scoring systems.[19,27] In a MASLD cohort, indices computed from SHG parameters were able to better predict clinical endpoints, including all-cause mortality, decompensation episodes, and HCC, compared to semi-quantitative fibrosis stages.[28] In AILD, the quantification of fibrosis has not been so extensively studied. A study of collagen proportionate area on liver explants showed how fibrosis in AIH and PSC compared to other etiologies.[29] More recently, collagen proportionate area was found to be predictive of clinical endpoints in
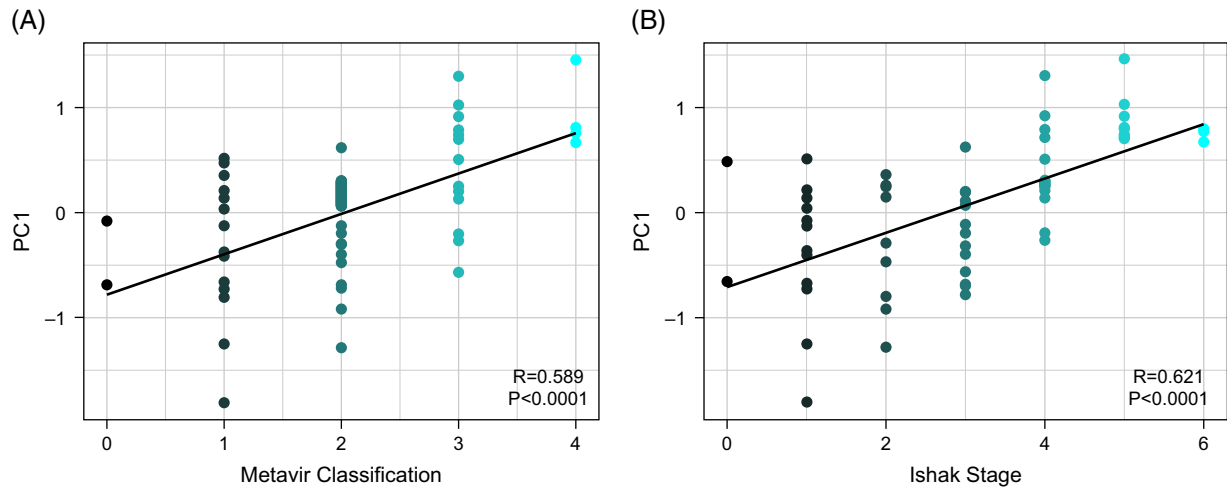
FIGURE 3 SHG/AI analysis of fibrosis and histopathologic staging of fibrosis. The principal component 1 is highly correlated ($p < 0.0001$) with both Metavir classification (A) and Ishak stage (B) according to Spearman correlation analysis. Abbreviations: AI, artificial intelligence; SHG, second harmonic generation.

PSC.[30] Yet, collagen proportionate area still relies on staining and has been described to perform less well than SHG/TPEF microscopy in animal models.[31] In primary biliary cholangitis, SHG/TPEF microscopy demonstrated that treatment with obeticholic acid was associated with a reduction in fibrosis.[32] To our knowledge, our study is the first to describe the use of SHG/TPEF microscopy in pediatric AILD.

AILD is a group of diseases with significant overlap, rendering classification challenging. On histology, Di Giorgio et al[33] showed that most children with AIH and ASC had at least moderate bile duct injury, with no difference between groups, and about half had some evidence of periductal fibrosis, although greater in the ASC group. They concluded both diseases were challenging to discern based on histology alone. Quantitative fibrosis can aid in distinguishing subtypes of AILD. We were able to discriminate 2 groups of patients based on greater total fibrosis and biliary tract involvement, revealing one with more patients with
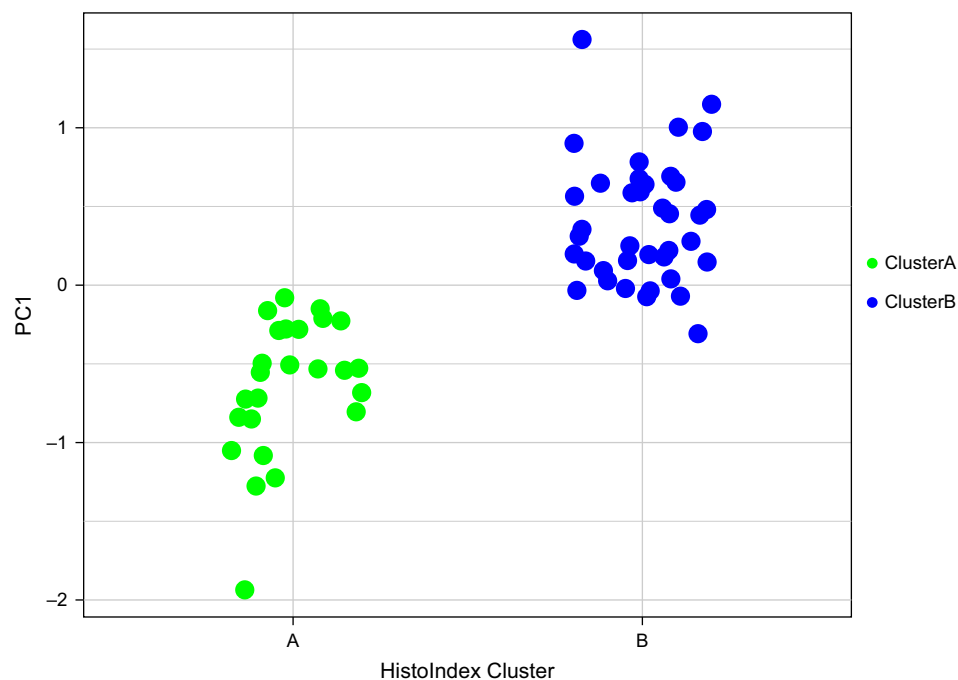
FIGURE 4 The PC1 segregates the AILD cohort into 2 clusters. The PC1 is strongly associated with hierarchical clusters A and B ($p < 0.0001$). The qFibrosis variables that comprised PC1 are the dominant variables directing subject clustering into hierarchical clusters A and B (Figure 1), indicating that overall and portal tract fibrosis may be most relevant in segregating phenotypes. Abbreviations: AILD, autoimmune liver disease; PC1, principal component 1.

TABLE 4 Predicting outcomes based on the principal component 1

Outcome	OR or HR (95% CI)	p
Abnormal ALT at 12 mo	3.6 (1.3, 10)	**0.01**
Abnormal AST at 12 mo	3.8 (1.5, 9.8)	**0.005**
Abnormal GGT at 12 mo	1.8 (0.8, 4.2)	0.16
Abnormal ALP at 12 mo	1.5 (0.5, 4.3)	0.43
Any liver complication	3.2 (1.3, 7.9)	**0.01**
Liver transplant	20.1 (3, 135.7)	**0.002**

Bold values are Statistical significance of p value.

Note: Abnormal biochemistries at 12 months were analyzed by logistic regression (reported as OR), whereas long-term outcomes were analyzed by Cox proportional hazards regression (reported as HR).

PSC/ASC. Patients with ASC have been shown to have a poorer prognosis than patients with AIH.[34,35] Children and adolescents with evidence of ASC have nearly a 3 times greater risk of liver transplant or mortality.[36] Similarly, in our study, a diagnosis of PSC/ASC was associated with less favorable clinical outcomes. Moreover, the grouping of ASC with PSC could support that these diseases are more similar in natural history than AIH, as recently suggested by Ricciuto et al.[37]

A pattern of greater overall and periportal fibrosis was found to be associated with nonresponsive disease and poorer clinical outcomes with a higher risk of liver transplantation. Normalization of ALT is clinically important and a therapeutic endpoint recommended by consensus guidelines as a marker of remission.[13] In AIH, not attaining biochemical remission increases patients' risk for liver transplantation or death.[36,38] Abnormal ALT levels are associated with ongoing histologic activity.[39] Residual activity on biopsy has been described to be associated with all-cause mortality and liver transplantation, while evidence of histologic remission is a predictor of reduction in hepatic fibrosis.[40,41] Moreover, the time over which patients respond to therapy is important as biochemical remission by 12 months is associated with a lower likelihood of evolving to cirrhosis in comparison to a more delayed response.[42] In our study, the degree of periportal and overall fibrosis by SHG was associated with persistently abnormal ALT at 12 months, possibly reflecting the relationship between ongoing inflammatory burden and the fibrosis it drives. It may also capture the subgroup of patients with biliary involvement, which is often not responsive to immuno-suppressive therapy in PSC and ASC. Indeed, as shown in several follow-up studies, transaminases normalize in a smaller proportion of patients with ASC when compared to those with AIH.[33,43,44]

The limitations of this study include that it was a single-center study. Despite having a reasonable population size for a pediatric cohort, our results should be validated in a larger multicenter study. In addition, SHG/TPEF microscopy with AI analysis is a technology that is not currently readily available for routine use, although it is under study in many hepatic diseases and its role is forthcoming.

The application of SHG/AI algorithms in pediatric-onset AILD improves the performance of liver histopathology. Quantitative fibrosis allows to objectively identify patients at greater risk of refractory liver disease and is associated with meaningful clinical endpoints that include liver-related complications and liver transplantation. Although a multicenter study is needed to confirm our findings, we suggest that SHG qFibrosis parameters could be used as potential tissue-based biomarkers for disease stratification and surrogate endpoints in pediatric-onset AILD.

AUTHOR CONTRIBUTIONS

Data extraction and interpretation: Leticia Khendek, Cyd Castro-Rojas, Constance Nelson, Mosab Alquraish, and Amy E. Taylor; pathology review and interpretation: Jennifer Kasten; statistical analysis: Rebekah Karns; drafting: Leticia Khendek, Alex G. Miethke, and Amy E. Taylor; and final revision: all authors.

FUNDING INFORMATION

CONFLICTS OF INTEREST

Xiao Teng is employed by and owns stock in HistoIndex. Alexander G. Miethke consults and received grants from Mirum Pharmaceuticals. The remaining authors have no conflicts to report.

ORCID

Leticia Khendek https://orcid.org/0000–0001–7903–5561
Constance Nelson https://orcid.org/0009–0005–6069–7748
Rebekah Karns https://orcid.org/0009–0007–0259–4550
Jennifer Kasten https://orcid.org/0000–0001–6439–9872
Alexander G. Miethke https://orcid.org/0000–0003–1395–9475
Amy E. Taylor https://orcid.org/0000–0001–5010–8157

REFERENCES

1. Maggiore G, Bernard O, Mosca A, Ballot E, Johanet C, Jacquemin E. Long-term outcomes of patients with type 1 or 2 autoimmune hepatitis presenting in childhood. J Hepatol. 2023; 78:979–88.

2. Deneau M, Jensen KM, Holmen J, Williams MS, Book LS, Guthery SL. Primary sclerosing cholangitis, autoimmune hepatitis, and overlap in Utah children: Epidemiology and natural history. Hepatology. 2013;58:1392–400..

3. Gregorio GV, Portmann B, Reid F, Donaldson PT, Doherty DG, McCartney M, et al. Autoimmune hepatitis in childhood: A 20-year experience. Hepatology. 1997;25:541–7.

4. Saadah OI, Smith AL, Hardikar W. Long-term outcome of autoimmune hepatitis in children. J Gastroenterol Hepatol. 2001;16:1297–302.

5. Gregorio G. Autoimmune hepatitis/sclerosing cholangitis overlap syndrome in childhood: A 16-year prospective study. Hepatology. 2001;33:544–53.

6. Deneau MR, El-Matary W, Valentino PL, Abdou R, Alqoaer K, Amin M, et al. The natural history of primary sclerosing cholangitis in 781 children: A multicenter, international collaboration. Hepatology. 2017;66:518–27.

7. Chazouilleres O, Beuers U, Bergquist A, Karlsen TH, Levy C, Samyn M, et al. EASL Clinical Practice Guidelines on sclerosing cholangitis. J Hepatol. 2022;77:761–806.

8. Ponsioen CY, Chapman RW, Chazouillères O, Hirschfield GM, Karlsen TH, Lohse AW, et al. Surrogate endpoints for clinical trials in primary sclerosing cholangitis: Review and results from an International PSC Study Group consensus process. Hepatology. 2016;63:1357–67.

9. Deneau MR, Mack C, Abdou R, Amin M, Amir A, Auth M, et al. Gamma glutamyltransferase reduction is associated with favorable outcomes in pediatric primary sclerosing cholangitis. Hepatol Commun. 2018;2:1369–78.

10. Karlsen TH, Folseraas T, Thorburn D, Vesterhus M. Primary sclerosing cholangitis—A comprehensive review. J Hepatol. 2017;67:1298–323.

11. Gilligan LA, Trout AT, Lam S, Singh R, Tkach JA, Serai SD, et al. Differentiating pediatric autoimmune liver diseases by quantitative magnetic resonance cholangiopancreatography. Abdom Radiol (NY). 2020;45:168–76.

12. Patil K, Ricciuto A, Alsharief A, Al-Rayahi J, Amirabadi A, Church PC, et al. Magnetic resonance cholangiopancreatography severity predicts disease outcomes in pediatric primary sclerosing cholangitis: A reliability and validity study. Hepatol Commun. 2020;4:208–18.

13. Mack CL, Adams D, Assis DN, Kerkar N, Manns MP, Mayo MJ, et al. Diagnosis and management of autoimmune hepatitis in adults and children: 2019 practice guidance and guidelines from the American Association for the Study of Liver Diseases. Hepatology. 2020;72:671–722.

14. Chang PE, Goh GBB, Leow WQ, Shen L, Lim KH, Tan CK. Second harmonic generation microscopy provides accurate automated staging of liver fibrosis in patients with non-alcoholic fatty liver disease. PLoS One. 2018;13:e0199166.

15. Gailhouste L, Grand YL, Odin C, Guyader D, Turlin B, Ezan F, et al. Fibrillar collagen scoring by second harmonic microscopy: A new tool in the assessment of liver fibrosis. J Hepatol. 2010;52:398–406.

16. Sun W, Chang S, Tai DCS, Tan N, Xiao G, Tang H, et al. Nonlinear optical microscopy: Use of second harmonic generation and two-photon microscopy for automated quantitative liver fibrosis studies. J Biomed Opt. 2008;13:064010.

17. Soon G, Wee A. Updates in the quantitative assessment of liver fibrosis for nonalcoholic fatty liver disease: Histological perspective. Clin Mol Hepatol. 2021;27:44–57.

18. Hsiao CY, Teng X, Su TH, Lee PH, Kao JH, Huang KW. Improved second harmonic generation and two-photon excitation fluorescence microscopy-based quantitative assessments of liver fibrosis through auto-correction and optimal sampling. Quant Imaging Med Surg. 2021;11:351–61.

19. Naoumov NV, Brees D, Loeffler J, Chng E, Ren Y, Lopez P, et al. Digital pathology with artificial intelligence analyses provides greater insights into treatment-induced fibrosis regression in NASH. J Hepatol. 2022;77:1399–409.

20. Hennes EM, Zeniya M, Czaja AJ, Parés A, Dalekos GN, Krawitt EL, et al. Simplified criteria for the diagnosis of autoimmune hepatitis. Hepatology. 2008;48:169–76.

21. Bedossa P, Poynard T. An algorithm for the grading of activity in chronic hepatitis C. The METAVIR Cooperative Study Group. Hepatology. 1996;24:289–93.

22. Ishak KG. Chronic hepatitis: Morphology and nomenclature. Mod Pathol. 1994;7:690–713.

23. Ishak K, Baptista A, Bianchi L, Callea F, De Groote J, Gudat F, et al. Histological grading and staging of chronic hepatitis. J Hepatol. 1995;22:696–9.

24. Wang TH, Chen TC, Teng X, Liang KH, Yeh CT. Automated biphasic morphological assessment of hepatitis B-related liver fibrosis using second harmonic generation microscopy. Sci Rep. 2015;5:12962.

25. Soon GST, Liu F, Leow WQ, Wee A, Wei L, Sanyal AJ. Artificial intelligence improves pathologist agreement for fibrosis scores in nonalcoholic steatohepatitis patients. Clin Gastroenterol Hepatol. 2023;21:1940–42.e3.

26. Davison BA, Harrison SA, Cotter G, Alkhouri N, Sanyal A, Edwards C, et al. Suboptimal reliability of liver biopsy evaluation has implications for randomized clinical trials. J Hepatol. 2020; 73:1322–32.

27. Ratziu V, Francque S, Behling CA, Cejvanovic V, Cortez-Pinto H, Iyer JS, et al. Artificial intelligence scoring of liver biopsies in a phase ii trial of semaglutide in non-alcoholic steatohepatitis. Hepatology. 2023;80:173–85.

28. Kendall T, Tai D, Ho G, Ren Y, Chng E, Fallowfield J. Digital pathology using stain-free imaging indices allows direct prediction of all-cause mortality, hepatic decompensation and hepatocellular carcinoma development in patients with non-alcoholic fatty liver disease. J Hepatol. 2023;78:S70–1.

29. Hall A, Germani G, Isgrò G, Burroughs AK, Dhillon AP. Fibrosis distribution in explanted cirrhotic livers. Histopathology. 2012;60: 270–7.

30. Saffioti F, Hall A, de Krijger M, Verheij J, Hübscher SG, Maurice J, et al. Collagen proportionate area correlates with histological stage and predicts clinical events in primary sclerosing cholangitis. Liver Int. 2021;41:2681–92.

31. Liu F, Chen L, Rao HY, Teng X, Ren YY, Lu YQ, et al. Automated evaluation of liver fibrosis in thioacetamide, carbon tetrachloride, and bile duct ligation rodent models using second-harmonic generation/two-photon excited fluorescence microscopy. Lab Invest. 2017;97:84–92.

32. Bowlus CL, Pockros PJ, Kremer AE, Parés A, Forman LM, Drenth JPH, et al. Long-term obeticholic acid therapy improves histological endpoints in patients with primary biliary cholangitis. Clin Gastroenterol Hepatol. 2020;18:1170–78.e6.

33. Di Giorgio A, D'Adda A, Marseglia A, Sonzogni A, Licini L, Nicastro E, et al. Biliary features in liver histology of children with autoimmune liver disease. Hepatol Int. 2019;13:510–8.

34. Al-Chalabi T, Portmann BC, Bernal W, McFarlane IG, Heneghan MA. Autoimmune hepatitis overlap syndromes: An evaluation of treatment response, long-term outcome and survival. Aliment Pharmacol Ther. 2008;28:209–20.

35. Czaja AJ. Frequency and nature of the variant syndromes of autoimmune liver disease. Hepatology. 1998;28:360–5.

36. Porta G, de Carvalho E, Santos JL, Gama J, Bezerra JA, Borges CV, et al. Autoimmune hepatitis: Predictors of native liver survival in children and adolescents. J Pediatr. 2021;229: 95–101.e3.

37. Ricciuto A, Kamath BM, Hirschfield GM, Trivedi PJ. Primary sclerosing cholangitis and overlap features of autoimmune hepatitis: A coming of age or an age-ist problem. J Hepatol. 2023;79:567–75.

38. Ngu JH, Gearry RB, Frampton CM, Stedman CAM. Predictors of poor outcome in patients with autoimmune hepatitis: A population-based study. Hepatology. 2013;57:2399–406.

39. Lüth S, Herkel J, Kanzler S, Frenzel C, Galle PR, Dienes HP, et al. Serologic markers compared with liver biopsy for monitoring disease activity in autoimmune hepatitis. J Clin Gastroenterol. 2008;42:926–30.

40. Dhaliwal HK, Hoeroldt BS, Dube AK, McFarlane E, Underwood JCE, Karajeh MA, et al. Long-term prognostic significance of persisting histological activity despite biochemical remission in autoimmune hepatitis. Am J Gastroenterol. 2015; 110:993–9.

41. Hartl J, Ehlken H, Sebode M, Peiseler M, Krech T, Zenouzi R, et al. Usefulness of biochemical remission and transient elastography in monitoring disease course in autoimmune hepatitis. J Hepatol. 2018;68:754–63.

42. Czaja AJ. Rapidity of treatment response and outcome in type 1 autoimmune hepatitis. J Hepatol. 2009;51:161–7.

43. Singh H, Balouch F, Noble C, Lewindon P. Evolving practice and changing phenotype in pediatric autoimmune liver disease: Outcomes from an Australian center. J Pediatr Gastroenterol Nutr. 2018;67:80–5.

44. Jiménez-Rivera C, Ling SC, Ahmed N, Yap J, Aglipay M, Barrowman N, et al. Incidence and characteristics of autoimmune hepatitis. Pediatrics. 2015;136:e1237–48.